



Deposited via The University of York.

White Rose Research Online URL for this paper:

<https://eprints.whiterose.ac.uk/id/eprint/89459/>

Version: Accepted Version

Article:

Hodge, Victoria J., Krishnan, Rajesh, Austin, Jim et al. (2014) Short-term prediction of traffic flow using a binary neural network. *Neural computing & applications*. 1639–1655. ISSN: 0941-0643

<https://doi.org/10.1007/s00521-014-1646-5>

Reuse

Items deposited in White Rose Research Online are protected by copyright, with all rights reserved unless indicated otherwise. They may be downloaded and/or printed for private study, or other acts as permitted by national copyright laws. The publisher or other rights holders may allow further reproduction and re-use of the full text version. This is indicated by the licence information on the White Rose Research Online record for the item.

Takedown

If you consider content in White Rose Research Online to be in breach of UK law, please notify us by emailing eprints@whiterose.ac.uk including the URL of the record and the reason for the withdrawal request.

Short-Term Prediction of Traffic Flow Using a Binary Neural Network

Victoria J. Hodge^a, Rajesh Krishnan^b, Jim Austin^a, John Polak^b, Tom Jackson^a

^a*Dept of Computer Science, University of York, York, UK*

^b*Centre for Transport Studies, Imperial College London, London, UK*

{victoria.hodge@york.ac.uk, rajesh.k@imperial.ac.uk, jim.austin@york.ac.uk, j.polak@imperial.ac.uk, tom.jackson@york.ac.uk}

Abstract.

This paper introduces a binary neural network-based prediction algorithm incorporating both spatial and temporal characteristics into the prediction process. The algorithm is used to predict short-term traffic flow by combining information from multiple traffic sensors (spatial lag) and time-series prediction (temporal lag). It extends previously developed Advanced Uncertain Reasoning Architecture (AURA) k-nearest neighbour (k-NN) techniques. Our task was to produce a fast and accurate traffic flow predictor. The AURA k-NN predictor is comparable to other machine learning techniques with respect to recall accuracy but is able to train and predict rapidly. We incorporated consistency evaluations to determine if the AURA k-NN has an ideal algorithmic configuration or an ideal data configuration or whether the settings needed to be varied for each data set. The results agree with previous research in that settings must be bespoke for each data set. This configuration process requires rapid and scalable learning to allow the predictor to be setup for new data. The fast processing abilities of the AURA k-NN ensure this combinatorial optimisation will be computationally feasible for real-world applications. We intend to use the predictor to proactively manage traffic by predicting traffic volumes to anticipate traffic network problems.

Keywords - *binary neural network; associative memory; k-nearest neighbour; time series; spatio-temporal; prediction*

Nomenclature

Variable = one feature of a traffic data vector, for example the flow value from a sensor.

Attribute = one time slice of one variable, for example the flow value from a sensor five minutes ago.

The final publication is available at Springer via <http://dx.doi.org/10.1007/s00521-014-1646-5>

1 Introduction

Intelligent Decision Support (IDS) systems are an important computerised tool in many problem domains. It is essential that any decision support system provides “intelligence” to help with good decision making. IDS systems are used to analyse information, establish models and support the decision making process. An IDS is predicated on providing a supportive role rather than entirely replacing humans in the decision-making process [1]. IDS has developed incorporating aspects from a broad spectrum of domains such as: expert systems; artificial intelligence; database technologies and, data mining and knowledge discovery.

The aim of our work is to provide an IDS tool to assist traffic network operators to optimally manage traffic as a part of the FREEFLOW project [2]. This tool aims to use neural-network-based pattern matching techniques to provide short-term predictions of traffic volumes to the traffic operators and thus help them to select the most appropriate course of action. The proposed IDS tool needs to operate in near “real time” and dynamically; providing predictions prior to the next data collection, where traffic data are updated every 5-15 minutes. Traffic monitoring and control systems produce large volumes of data which infers that traditional relational databases are not suitable for online traffic applications such as the IDS. Also, traffic data distributions are frequently non-stationary; hence, any method needs to be able to accommodate non-stationary data while still maintaining fast, flexible processing. The proposed methodology could be extended to other monitoring applications that use spatially distributed sensors where neighbourhoods of sensors exist and where temporal characteristics are important.

In the remainder of this paper, we provide a concise review of traffic flow and neural network-based prediction methods in section 2, section 3 discusses our proposed binary neural network predictor, sections 4 provides an evaluation of our proposed prediction method against alternative machine learning methods. The evaluation analyses the prediction accuracy; and examines whether there is a single algorithm configuration and whether there is a single data configuration that performs best with respect to prediction accuracy. The evaluation is focused on the timing analyses of the training and the execution time of our proposed technique. We then analyse the results of the evaluations in section 5 and provide our conclusions in section 6.

2 Short-term Prediction

The focus of our work in this paper was to predict future traffic flows over short-term intervals using time series prediction [3]. The predicted flow may then be displayed to the

traffic operator to allow them to visualise how the traffic will develop over the near future and to anticipate traffic problems. We provide a selective review of time series prediction literature with particular reference to vehicle flow prediction and neural network-based predictors.

Well-known short-term prediction algorithms can broadly be classified into univariate and multivariate approaches. Simple univariate prediction models predict the value of a variable as a function of the same variable observed in the immediate past. Ding et al. [4] used support vector machines [5] to model future traffic flows at a given location as a function of past flow observations at the same location. The ARIMA methodology introduced by Box and Jenkins [6] is a popular statistical approach for time series prediction. Hamed and Al-Masaeid [7] used an ARIMA time-series model to predict 1-minute future traffic flows. Williams et al. [8] added seasonal differencing to the ARIMA model to predict 15-minute-ahead flows with a periodicity of 24-hours. More recently, Ghosh et al. [9] used a seasonal ARIMA model calibrated using Bayesian methods to predict traffic flows. However, the ARIMA method requires time consuming manual configuration for each problem scenario to obtain accurate prediction results. In addition, it is not easy to incorporate additional explanatory variables other than the observed variable in the ARIMA framework.

In contrast, a multivariate approach uses data from several locations for traffic prediction. The traffic flow on a road network is a spatial-temporal process. The traffic variables observed at a given location are correlated with the present and past values of the same traffic variables observed at upstream or downstream locations. Hence, traffic prediction models often use observations from neighbouring sensor locations as explanatory variables to predict the value of a sensor variable at a given location.

Neural networks are often used for traffic variable prediction but many neural networks require intensive tuning to ensure optimal performance. Amin et al. [10] used a Radial Basis Function (RBF) neural network to perform traffic flow prediction. In an IDS application, the neural network would need to be retrained every time new data became available which is likely to be daily. It is also likely that different parameter sets would be required for different locations on the road network. This training and retraining introduces high computational complexity. For example, Vlahogianni et al., [11] demonstrated a genetic algorithm for optimising Multi-Layer Perceptrons (MLPs) with respect to the learning settings and the hidden layer topology. The optimised neural network was then used for short-term traffic flow prediction. Abdulhai et al. [12] demonstrated a similar approach for traffic flow prediction by using genetic algorithms to tune neural networks but the underlying MLP incorporated temporal lag by using

multiple links between neurons. These additional links introduced a time delay between network layers to capture the evolution of vehicle flow over time.

Martinetz et al. [13] used the neural gas network for chaotic time series prediction. Neural gas extends both k-means clustering and Kohonen neural networks. Predictions are generated from learning input to output mappings where the output is the future value associated with the training example (input value). Zhang et al. [14] developed a Bayesian network model to describe the traffic flows. Their approach used a Gaussian Mixture Model to approximate the joint probability distribution within the Bayesian network nodes following dimensionality reduction by Principal Component Analysis.

Kindzerske and Ni [15] are one of a number of authors to realise Yakowitz's [16] developmental work by applying non-parametric regression, the k-NN algorithm, to time series prediction. Kindzerske and Ni [15] represented the current snapshot of the traffic sensors as a vector and compared this vector against historical vectors. The best matching historical vectors are then combined to generate a prediction. Krishnan and Polak [17] enhanced this by introducing temporal lag in their k-NN approach so that each of the sensor's variables formed a time series and the set of all time-series were concatenated to produce a vector covering the spatial distribution of sensors.

In a similar manner, Kamarianakis and Prastacos [18] introduced a spatio-temporal extension of ARIMA to predict future flows as a function of historical flows from a given location and its upstream locations.

The accuracy of prediction depends on both the appropriateness of the data configuration and the correct implementation of the machine learning tool. For spatio-temporal data, simply incorporating spatially distributed sensors and attributes may actually generate predictions that are worse than non-spatial models unless the data from these neighbouring locations influence the predicted value. Kamarianakis and Prastacos [18] showed that injudicious use of data from neighbouring locations may actually decrease prediction accuracy. They showed that using relatively few, dispersed sensors fails to account for the spatial dependencies. Conversely, they found that as the number of sensors increases, the prediction accuracy may improve significantly if spatio-temporal relationships are captured.

To summarise, traffic prediction models need to (1) accurately model historical traffic flow patterns, (2) account for both the intra-day and inter-day variability in traffic variables, (3) be able to incorporate both temporally and spatially distributed information, where appropriate, to improve prediction accuracy and (4) generate predictions rapidly between data collections.

2.1 Our approach

In this paper, we develop a fast and scalable neural network-based k-NN predictor implemented using the AURA binary neural architecture. It is adapted from the methodology described in [17] which incorporated temporal and spatial lag into standard k-NN traffic flow prediction.

- The AURA k-NN has only previously been described for non-temporal data. In this paper, we extend the AURA k-NN method to encompass time series processing. Traffic data change over time which necessitates a temporal component for prediction.
- The AURA k-NN has also only been used previously for pattern match so we extend the AURA k-NN to produce multivariate short-term predictions to allow future traffic flows to be estimated.

The resultant method predicted future traffic flows by matching a current time series pattern against historical data patterns and using these matching time series to predict either how the current traffic state will develop over time or what may happen if a particular control mechanism is implemented. The methodology described is fast, flexible and satisfies the four criteria above. It also has wider application to other time series prediction tasks, beyond the prediction problem addressed in this paper, for example, [19], [20].

3 Binary Neural Network for prediction

The objective for the neural network-based pattern matching method was to predict the future traffic flows to allow the traffic operator to visualise how the traffic situation will develop. The AURA k-NN method identified a set of historical time periods when the set of traffic observations on the road network were most similar to the current observations. It then used this information to produce a prediction of the future traffic flow by averaging the flow development across the set of matches.

3.1 AURA k-NN

K-NN is a nonparametric pattern matching technique known to be robust and flexible and allows the predictor to be updated continuously. However, a drawback of conventional k-NN is its speed, as it becomes very slow for large problems. This drawback is overcome by using the AURA neural network technique to underpin the k-NN. Using AURA means that the AURA k-NN can perform up to four times faster than the standard k-NN [21]. AURA is a group of techniques designed for high speed search and match operations in large data sets. The foundation of AURA is a binary Correlation

Matrix Memory (CMM): a binary matrix used to store and retrieve patterns [22]. In the AURA k-NN developed previously [21, 23, 24, 25], each column of the CMM was a set of attribute observations for a record (pattern) and each row indexed an attribute value or a quantised range of values. AURA applies input patterns to the CMM to act as a cue to retrieve similar output patterns. We extended the approach to match time-series vectors and then to generate short-term predictions in this paper. The details of the AURA k-NN implementation are given in the following text.

3.1.1 Time Series

In the traffic domain, the AURA k-NN can process a broad spectrum of traffic variables such as vehicle counts, vehicle speeds, bus timetable adherence, traffic signal settings, congestion metrics, roadworks data, events data, and weather data. In this paper, we used flow and occupancy data from sensors located in the roads. Flow is the number of vehicles passing over the sensor during unit time and occupancy is the percentage of time vehicles are present over the sensor during a specific time period.

For traffic prediction, the system must incorporate time: traffic data are dynamic and show recurring patterns with respect to time. We describe how we accommodated temporal aspects into the pattern match.

Given the current set of observations, X_n , from the set of traffic sensors and a dataset of historical records $\{X\}$, k-NN identifies the k nearest neighbours of X_n in $\{X\}$ using a distance metric. In this paper, the data records were time-series representations of spatially distributed sensors to incorporate trend similarity and spatial awareness into the prediction approach. To produce the time series, the AURA k-NN effectively buffered historical data and accumulated data for a preset time interval, PT . It always preserved the temporal ordering of the data, thus, $Buffer_v = \{Buffer_{vt} : t \in PT\}$ represents the time series buffer of variable v of the data. The time-series for record X_n which we call X_n^{TS} becomes equation 1:

$$X_n^{TS} = \{X_{1t-3}, X_{1t-2}, X_{1t-1}, X_{1t}, X_{2t-3}, X_{2t-2}, \dots, X_{nt-3}, X_{nt-2}, X_{nt-1}, X_{nt}\} \quad (1)$$

for PT of four time lags $\{t-3, t-2, t-1, t\}$. The results of our evaluations in section 4 show that the number of time lags needs to be tuned for each data set.

For example, for two sensors reporting two variables: flow and occupancy, where sensor₁ has readings of 51, 62, 55, 68 for flow and readings of 15.0, 18.0, 21.0, 29.0 for occupancy for four time lags $\{t-3, t-2, t-1, t\}$ respectively and sensor₂ has flow readings of 38, 38, 56, 58 and occupancy readings of 15.0, 16.0, 23.0, 25.0 respectively, then X_n^{TS} is given in equation 2:

$$X_n^{TS} = \{51, 62, 55, 68, | 15.0, 18.0, 21.0, 29.0, | 38, 38, 56, 58, | 15.0, 16.0, 23.0, 25.0\} \quad (2)$$

where the vertical bars illustrate the sections of the pattern with each section representing the time series buffer for one sensor variable (flow or occupancy here).

3.1.2 Learning

The CMM is used in AURA to store representations of all data. The CMM is an $m \times n$ binary matrix that learns the N records in the data set. During learning, the CMM forms an association between an input pattern and an output pattern $I_n \rightarrow O_n$ for each record n where I_n and $O_n \in \{0,1\}$ as shown in figure 1.

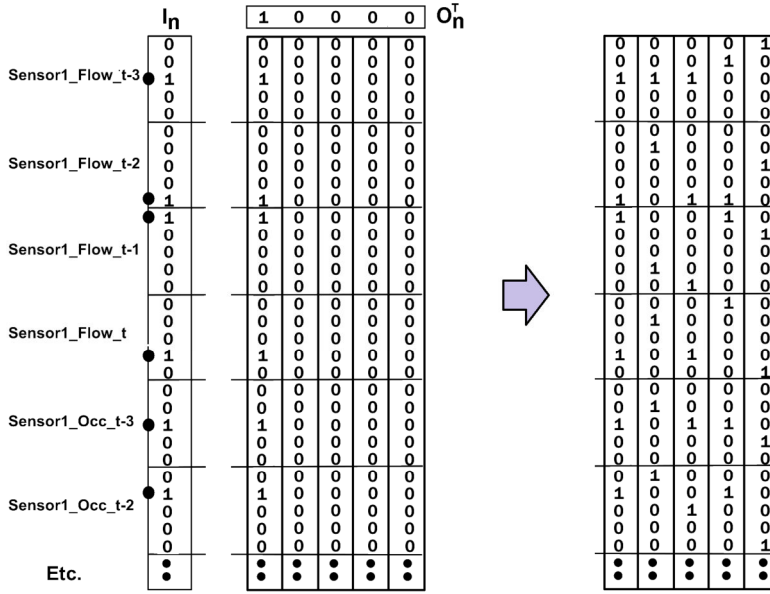


Figure 1. Showing the CMM storing the first association $I_0 \times O_0$ on the left and a CMM trained with five associations on the right.

The input pattern (I_n) represents the concatenated set of all time-series buffer values for all variables of a particular record X_n^{TS} and indexes matrix rows. In the remainder of this paper, each value of each time series buffer of each variable is referred to as an attribute. There are 16 attributes in equation 2. The associated output vector (O_n) uniquely identifies that record and indexes the matrix columns. Thus, the set of attribute values for record n are associated with a unique identifier for the record. In figure 1, I_0 is stored in the leftmost column of the CMM and is uniquely indexed by O_0 (10000) which activates the leftmost column.

The CMMs require binary input patterns for computational efficiency while training and matching; so numeric attributes must be quantised (binned) to allow mapping to a binary pattern [21]. Quantisation maps a continuous-valued attribute into a smaller ("finite") set of discrete symbols or integer values. Each attribute is quantised over its full range of values and mapped to a set of bins. This allows each bin to index a specific and unique row in the CMM. For example, for an integer-valued attribute with range 0-99 and five bins then each bin would have width 20: $bin_0 \{0..19\}$, $bin_1 \{20..39\}$... $bin_4 \{80..99\}$.

For a real-valued attribute with range [0.0-100.0] and five bins then each bin would have width 20: bin_0 [0.0, 20.0), bin_1 [20.0, 40.0) ... bin_4 [80.0, 100.0]. Thus, for the sensor₁ and sensor₂ above, the set of bin mappings for X_n^{TS} in equation 2 are given in equation 3:

$$Bins(X_n^{TS}) = \{2, 3, 2, 3, | 0, 0, 1, 1, | 1, 1, 2, 4, | 0, 0, 1, 1\} \quad (3)$$

In the AURA k-NN, each bin index maps to a binary representation to generate the binary patterns for AURA. For an attribute with five bins, the five possible binary representations are: $bin_0 = 00001$, $bin_1 = 00010$, $bin_2 = 00100$ etc. To produce the input vector I_n to train into the CMM, the binary representations for all the attributes in the data pattern are concatenated. The bin indexes for all attributes in X_n^{TS} are set to 1 while all other bin indexes remain unset (0). The binary input vector I_n derived from the bin mappings in equation 3 is given in equation 4. This is the input learning pattern to be stored in the CMM to allow the particular association $I_n \times O_n$ to be stored and retrieved

$$I_n = \{00100 01000 00100 01000 | 00001 00001 00010 00010 | 00001 \dots\} \quad (4)$$

Each binary input pattern I_n is associated with a unique binary output pattern O_n which has a single bit set to index a single column in the CMM. This column thus uniquely indexes the binary pattern I_n . For example, O_0 (10000) uniquely indexes I_0 which is the leftmost column in figure 1.

The CMM stores an association for all N records in the data set $\{X^{TS}\}$. Thus, the CMM represents $\{(I_1 \times O_1), (I_2 \times O_2), \dots (I_n \times O_n)\}$. Learning is a one-pass process with one learning step for each record in the data set. Hence, training is rapid. CMM learning is given in equation 5.

$$CMM = \bigcup_{n=1}^N I_n \times O_n^T \quad \text{where } \cup \text{ is logical OR} \quad (5)$$

$I_n \times O_n^T$ is an estimation of the weight matrix $W(n)$ of the neural network as a linear associator. $W(n)$ forms a mapping representing the association described by the n th input/output pair. The CMM is then effectively an encoding of the N weight matrices W . Individual weights within the weight matrix update using a generalisation of Hebbian learning [26] where the state for each synapse (matrix element) is binary valued. Every synapse (matrix element) can update its weight independently and in parallel.

Each I_n has m bits set where m is the number of attributes (assuming no missing values) and each I_n is of length $m \cdot b$ where b is the number of bins per attribute. Each O_n has 1 bit set and has length N . There are N associations (one per data record). Therefore,

the CMM contains $m \times N$ set bits, i.e., $\frac{mN}{mbN} = \frac{1}{b}$ possible bits are set in the CMM after training. This allows a compact representation [27] to be used where each input pattern,

each output pattern and the CMM are represented by the indices of the set bits only. This

means that only $\frac{1}{b}$ indices need to be stored for the CMM. This is similar to the pointer representation used in associative memories [28]. This compact representation ensures that retrieval, as described next, is proportional to the number of set bits in both the retrieval pattern and the CMM and is fast and scalable.

3.1.3 Retrieving the best matches

During retrieval, the CMM is searched to find the k best matches. Each query record is of the same format as the records in the training data (see equation 2). For each new query X_q^{TS} , a retrieval pattern R is created. R is formed from a set of parabolic kernels, with one kernel for each attribute in X_q^{TS} . The kernels emulate Euclidean distance [21] to allow us to emulate standard (Euclidean) k-NN. For each time slice for a particular variable, the kernels are identical but they may vary across variables according to the number of bins assigned to that variable. For example, a flow variable may use a different number of bins compared to an occupancy variable. In this paper, all attributes use an equal number of quantisation bins and, hence, an equivalent kernel. The kernel density is estimated using equation 6 for all attributes a in X_q^{TS} and an example kernel is shown in figure 2.

$$Kernel(a) = \left[\left[\left(\frac{\max(b)}{2} \right) \right]^2 - \left(|bin(x_a^q) - bin(x_a^h)| \right)^2 \right] \alpha(x_a^q) \quad \text{where } \alpha(x_a^q) = \frac{(\max(b))^2}{(b(x_a^q))^2} \quad (6)$$

Where, $\max(b)$ is the maximum number of bins across all attributes, $|bin(x_a^q) - bin(x_a^h)|$ is the number of bins separating the bin mapped to by this attribute value for the query pattern (x_a^q) from the bin mapped to by this attribute value for the stored historical pattern (x_a^h), and $b(x_a^q)$ is the total number of bins for attribute x_a .

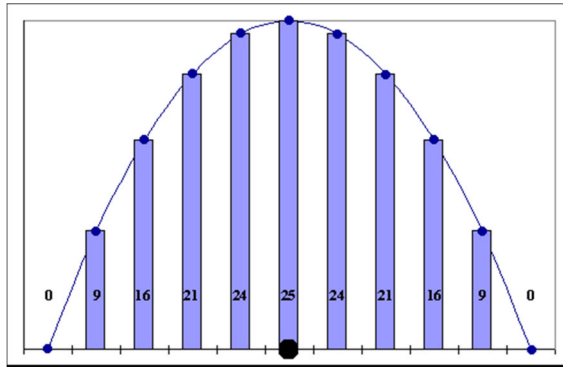


Figure 2. Showing the kernel values produced from equation 6 to approximate Euclidean Distance.

To emulate the scoring of Euclidean Distance, the kernels for all attributes are concatenated. Each kernel is centred on the bin representing that attribute's value in the

query record. This ensures that the query value itself receives the highest score and the score reduces according to the distance from the query value. For an integer-valued attribute with range 0-99 and five bins then each bin would have width 20: $bin_0 \{0..19\}$, $bin_1 \{20..39\}$... $bin_4 \{80..99\}$. Thus, if the query record value was 31 this would map to bin_1 so the input vector element representing bin_1 would be the centre of the kernel. The highest value for this kernel (analogous to the dotted value of the kernel in figure 2) would be centred on bin_1 .

For Euclidean kernels, the retrieval pattern input to the CMM to retrieve the top k matches is iteratively given by equation 7:

$$R' = R \oplus \text{offset}(\text{Kernel}(x_a)), \text{ for all attributes } x_a \quad (7)$$

where $\text{offset}()$ indexes attribute x_a 's section of the input pattern R and ensures that the kernel is added to R , centred on the query value for attribute x_a and \oplus is the concatenation operator. Thus, each attribute indexes a defined set of elements in R as shown in figure 3.

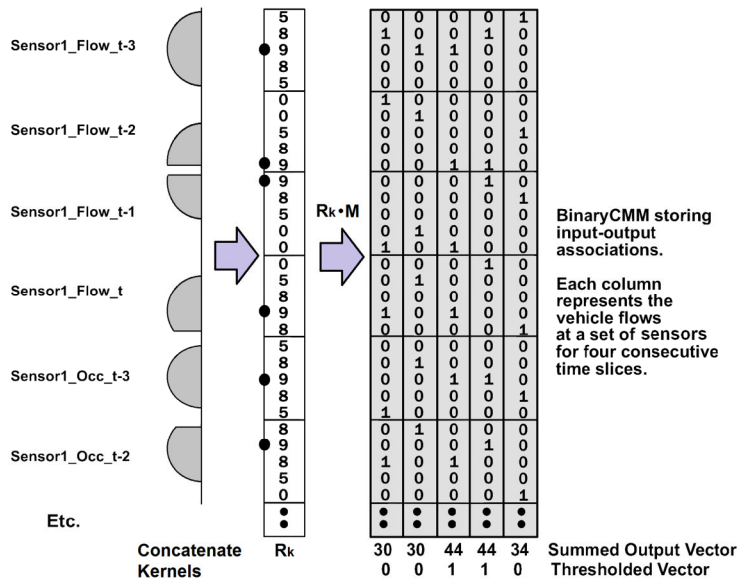


Figure 3. Illustrating the application of kernels to a CMM to find the k -nearest neighbours using time-series vectors. The kernels are mapped onto an integer vector R_k which is applied to the binary CMM by multiplying the CMM rows by the integer values. The CMM summed output vector is thresholded to retrieve the k best matches.

When R is applied to the CMM to retrieve the best matches, the values in R , multiply the rows of the matrix as shown in figure 3. If the bit is set to one in a particular column, then the column will receive the kernel score for the corresponding row as given in equations 7 and 8. The process is illustrated in figure 3. For Sensor1_Flow_t-3, columns 1 and 2 (indexing from 0 on the left) receive a score of 9 as the set bit in the respective columns aligns with the score of 9 in the input kernel. In contrast, the right column receives a score of 5 as the set bit in the right column aligns with the score of 5 in the input kernel.

To retrieve the best matching records, the columns (one column per record) of the matrix are summed according to the value on the rows indexed by the query input pattern R and the CMM produces a summed output vector S as given in Equation 8.

$$S^T = \sum R \bullet CMM \quad (8)$$

The summed output vector is then thresholded using L-Max thresholding [29] to produce a binary thresholded vector T . L-Max thresholding is used in the AURA k-NN as it retrieves the top L matches. After thresholding, T effectively lists the top L matching columns which represent the top k (where $k=L$) matches; i.e, the k nearest neighbours. This is also illustrated in figure 3.

The overall retrieval time is proportional to the number of set bits in both the retrieval vector and the CMM. If the retrieval vector is a binary vector, similar to I_n used in training, then retrieval from the CMM is a count of the number of exact matching binned attribute values for every stored record $n \in N$. If we assume that on average each stored vector (matrix column) matches 50% of the input and we assume the set bits are

equally distributed across the rows then only $\frac{mN}{2}$ bits are examined during retrieval where m is the number of attributes. We performed recall accuracy investigations using a number of different kernels for retrieval and using the Euclidean kernels significantly improves recall accuracy compared to other approaches [30]. However, the accuracy increase is at the expense of a slight speed decrease compared to using a single bit set pattern. The Euclidean kernel excites all CMM rows of the attribute if the kernel is centred on the middle bin and half of the rows if centred on one of the extreme value bins. If we assume that on average 75% of the rows are excited for each attribute and the bits

are equally distributed across the rows then $\frac{3mbN}{4}$ bits are examined during retrieval.

Thus, the kernel based AURA k-NN has runtime growth of $\Theta\left(\frac{3mbN}{4}\right)$ where $mb \ll N$ so this is approximately equal to growth proportional to $O(n)$ where n is the number of records.

3.1.4 Prediction

For the prediction task in this paper using data arriving at 15 minute intervals from the sensors, we retrieved the k top matches and then looked up the $t+1$ (+15 minute) or $t+4$ (+1 hour) sensor values for each of the k matches (these are stored in a database). The $t+1$ (+15 minute) prediction is then the mean value of the set of $t+1$ values from the k nearest neighbours and the $t+4$ (+1 hour) prediction is the mean of the $t+4$ values.

4 Evaluation

We evaluated our AURA k-NN prediction method against a number of predictors implemented using WEKA 3.6 software [31]. WEKA [32] is a Java GUI-based application that contains a set of machine learning algorithms designed for data mining. The algorithms can be used for tasks including data pre-processing, classification, prediction and clustering. Note WEKA prediction is to 3 decimal places whereas AURA predicts to integers to display to the traffic operator. The methods used were;

1. **Standard k-NN** [33] known as Instance Based learning (IBk) in WEKA 3.6 - we used $k=50$ and $k=10$ in our analyses.
2. **Multi-Layer Perceptron (MLP) Neural Networks** are feedforward supervised neural networks with at least one layer of nodes between the input nodes and output nodes. The network links flow forward from the input to the output layer. The network is trained by the backpropagation learning algorithm [34] using historical data. Training creates a model that maps inputs to outputs and this model can then be used to predict the output when new data is applied. MLPs have been used for traffic prediction on a number of occasions. For optimum results, the parameters of the MLP are intensively tuned; for example, using a genetic algorithm [11]. However, this intensive tuning process is too slow for an on-line application such as the IDS. Nevertheless, we ensured that we evaluated at least as many parameter sets for the MLP as we evaluated for the AURA k-NN. For all evaluations, the MLP used learning rate decay, train and validate (using 30% of the training data for validation) and we varied the key MLP parameters: learning rate and momentum. All other settings were WEKA defaults as these produced the best prediction accuracy. An example WEKA MLP configuration is listed in the Appendix showing the settings that we varied. Learning rate determines the amount the network weights are updated as training proceeds. Decaying the learning rate “may help to stop the NN from diverging from the target output as well as improve general performance”. Using a train and validate regime ensures that the training data are split between actual training data and validation data. Validation data are used to test the trained network and stop training before performance degrades.
3. **Support Vector Machine (SVM)** is implemented as SMOreg in WEKA 3.6 and implements the support vector machine for regression [31][35]. Support vector machines map the data to a high dimensional feature space and generate linear boundaries in the feature space to represent the non-linear class boundaries. SMOreg implements sequential minimal optimisation to train the support vector regression and all attributes are normalised. Again, we ensured that we evaluated at least as many parameter settings for the SVM as we evaluated for the AURA k-NN. The SVM used

an RBF kernel and we varied the complexity. Labeeuw et al. [36] assessed various machine learning techniques for the similar task of predicting traffic speeds and congestion. They concluded that SVMs with an RBF kernel had the highest accuracy of the methods evaluated so we used it here. All other settings were WEKA defaults as these produced the best prediction accuracy. An example WEKA SVM configuration is listed in the Appendix showing the settings that we varied.

4. **Least Median Squares (LMS) regression** – In WEKA, the LMS regression functions are generated from random subsamples of the data. The LMS regression with the lowest median squared error is then used as the final model. Our implementation used all default settings.

The performances of the various configurations of the AURA k-NN were compared against each other based on their prediction accuracy over an independent test set (out-of-sample accuracy) using the metrics in equations 9, 10 and 11. The MLP, SVM and LMS provided baseline accuracies to allow us to compare the standard k-NN and AURA k-NN prediction accuracies using the metric in equation 11.

$$\text{Mean Percentage Error (MPE)} = \frac{\sum_{i=1}^n \frac{X_i - F_i}{X_i} \times 100}{n} \quad (9)$$

- measures the bias (over-estimating or under-estimating)

$$\text{Mean Absolute Percentage Error (MAPE)} = \frac{\sum_{i=1}^n \left| \frac{X_i - F_i}{X_i} \times 100 \right|}{n} \quad (10)$$

- measures the goodness-of-fit

$$\text{Root Mean Squared Error (RMSE)} = \sqrt{\frac{\sum_{i=1}^n (X_i - F_i)^2}{n}} \quad (11)$$

- Measures the absolute error – this is the best metric for comparing different methods.

4.1 Data

In our application the IDS is required to run in near real-time so we need to minimise the data pre-processing. The only pre-processing performed was to clean the two data sets used using a simple rule: Univariate Screening given in Krishnan [37]. If a historical record contained an erroneous value then the entire record (one vector in the training set) was removed.

For the WEKA algorithms evaluated, the training data comprised the data vector as per equation 2 associated with the $t+x$ value for the sensor to be predicted (the class

value). For +15 minute prediction, the training vector was the vector from equation 2 with the $t+1$ sensor reading as the class value. Accordingly, for +1 hour prediction, the training vector was the vector from equation 2 with the $t+4$ sensor reading as the class value. To generate the prediction, the algorithm predicted the class value from the query data vector. The algorithms were tested using two traffic data sets from central London in Russell Square and Marylebone Road.

4.1.1 Data Set 1

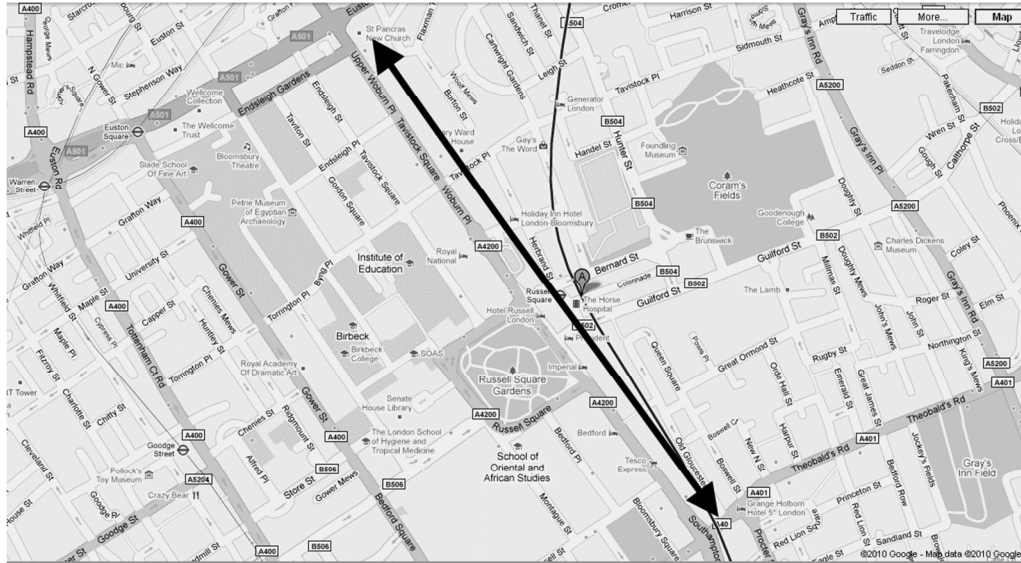


Figure 4. The Russell Square corridor in central London (Source: Google Maps).

Data from seven sensors arranged in series along the Russell Square corridor (southbound) in central London (see figure 4) was the first data set used for the prediction experiment in this paper. The flows on the southernmost (downstream) sensor were predicted. All sensors output two attributes: 15-minute flow values (which vary between 0-800) and 15 minute occupancy values (with data range 0.0-100.0). The data were obtained for the months of June, July and August 2007. Data from June and July were used as the training set and data for August formed the test set. The training and test data sets comprised only data from weekdays (Monday to Friday) with 3,840 training records and 337 query records after cleaning.

4.1.2 Data Set 2

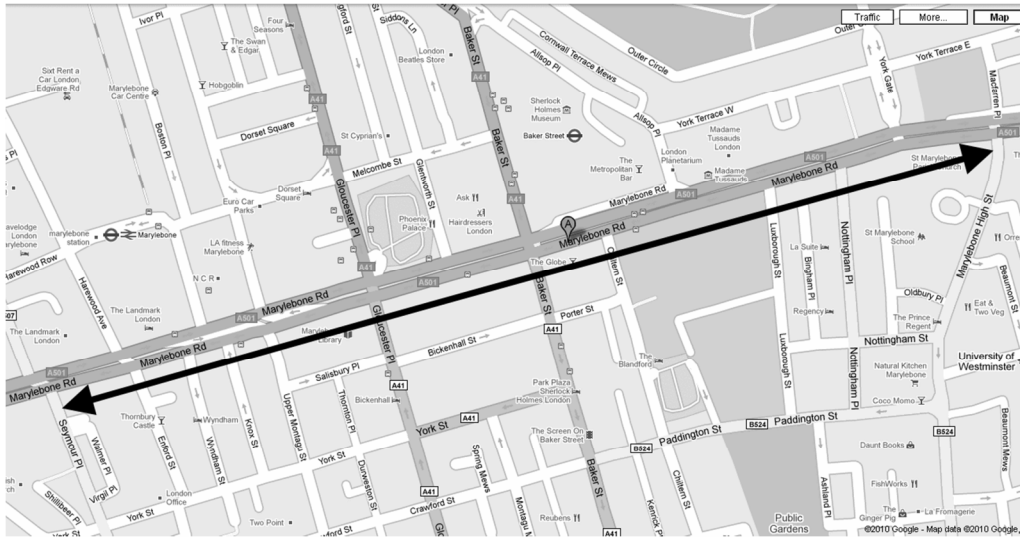


Figure 5. Marylebone Road in central London (Source: Google Maps).

Data set 2 comprised data from six sensors on Marylebone Road (eastbound) in central London (see figure 5) where the future flow values at the easternmost (downstream) sensor were predicted. The six sensors output 15-minute flow values with data range 0-1600. Training data were from May 2008 and 1st-13th June 2008 while test data were from 16th-20th June 2008 (one week). Only the weekday data were used giving 2,976 training records and 480 query records. A severe traffic incident happened in Marylebone Rd on 20th June from 18:59 to 21:01. We ran two analyses, one using all of the test data from 16th-20th June and a second analysing data from the 20th June, the day the incident occurred which comprised 96 records. The latter analysis provided an indication of how well the various machine learning techniques performed on incident data when the traffic flow would be anomalous and prediction is potentially more useful to end-users.

4.2 Tests

We ran seven separate tests to: find the best AURA k-NN parameter settings; pinpoint the best data configurations; compare the accuracy of the predictors; and, ultimately, evaluate the training and query time of the AURA k-NN. Parameter setting is a combinatorial search problem and both algorithmic and data-related parameters may be varied. Hence, we did not exhaustively test every possible parameter combination as this would be computationally intractable. Instead, we analysed a range of data and algorithm settings to evaluate both accuracy and consistency and whether we need to use bespoke settings for each data set. Tests 1-3 use data set 1: the data for Russell Sq. in June, July and August, 2007. Tests 4-7 use data set 2: the data for Marylebone Rd in May and June, 2008.

4.2.1 Test 1 – the best AURA k-NN configuration

This test was to investigate the best configuration with respect to the internal parameters of the AURA k-NN. These parameters were: the length of the time series (*TS*); the number of bins (*Bins*); and, the *k* value for k-NN (*k*). We varied the setting of the parameters in turn and counted the number of times each setting had the lowest RMSE across the evaluations of that parameter. The results are listed in table 1.

Table 1. Table with count of the number of times each AURA k-NN parameter setting has the lowest RMSE. The highest counts for *TS*, *Bins* and *k* are shown in bold.

	<i>TS</i>					<i>Bins</i>			<i>k</i>			
	2	4	6	8	10	11	25	49	10	25	50	100
RMSE – 15 mins	0	0	0	4	3	1	0	7	0	0	11	0
RMSE – 60 mins	0	0	0	5	2	6	0	2	0	4	7	0

The most consistent time series length and *k*-value are clear (*TS*=8 and *k*=50, respectively). The number of quantisation bins to use was less clear. When predicting +15 minutes, 49 quantisation bins performed best. When predicting +1 hour, 11 bins generally performed best as this has the highest winning count. However, the two best performing configurations for +1 hour with respect to both MAPE and RMSE use 49 bins rather than 11 bins.

Test 1 indicated that optimising the algorithm configuration was important and needed care.

4.3 Test 2 – the best data configuration

Test 1 evaluated the AURA k-NN settings so test 2 evaluated different data configurations to find the optimal data configuration(s) for prediction with AURA k-NN. In test 2, we used the best AURA k-NN configuration from test 1 (*TS*=8, *Bins*=49, *k*=50) and evaluated the following data settings: the number of sensors (*NS*) to use, whether to incorporate the attributes of the sensor, *self*, whose flow is being predicted (*S*) and whether to incorporate the occupancy attribute (*O*). All evaluations used the flow attribute (*F*). Each configuration was given a label to allow it to be referenced in the text. The results of test 2 are given in table 2.

Table 2 shows that there was a clear difference between the best and worst RMSE for both +15 minute and +1 hour prediction. Configurations 1-6 and 1-7 performed best with respect to both RMSE and MAPE.

From table 2, configurations 1-6 and 1-7 have higher MPE than the other configurations indicating that they overestimate more while the other configurations alternate between under and over estimations of larger magnitudes. The occupancy attribute contributed to one of the two best performing configurations but is not a

necessity as the other best performing configuration did not use occupancy. Including all sensors produced higher accuracy compared to limiting the number of sensors. Including the self-sensor improved accuracy with the flow attribute only but did not improve accuracy with both flow and occupancy attributes. Again, this indicates that the data need to be carefully configured.

Table 2. Table listing the MPE, MAPE and RMSE for the various data configurations of the AURA k-NN. 15 indicates +15 minute ahead prediction and 60 indicates + 1 hour ahead prediction. The highest prediction accuracy for each column is shown in bold.

<i>AURA k-NN Configuration</i>					<i>MPE</i>		<i>MAPE</i>		<i>RMSE</i>	
<i>Name</i>	<i>NS</i>	<i>S</i>	<i>F</i>	<i>O</i>	<i>15</i>	<i>60</i>	<i>15</i>	<i>60</i>	<i>15</i>	<i>60</i>
1-1	4	0	Y	N	-3.34	-3.36	12.6	15.2	65.7	77.9
1-2	4	0	Y	Y	-3.57	-3.01	12.8	15.4	66.0	77.7
1-3	4	1	Y	N	-2.95	-3.20	12.4	15.4	65.5	79.0
1-4	4	1	Y	Y	-3.18	-3.47	12.7	15.4	66.6	78.3
1-5	6	0	Y	N	-3.21	-3.95	12.5	14.9	65.5	76.1
1-6	6	0	Y	Y	-3.78	-3.41	12.5	14.8	65.3	75.3
1-7	6	1	Y	N	-3.35	-4.11	12.3	14.8	65.2	76.1
1-8	6	1	Y	Y	-3.89	-3.98	12.5	15.0	65.9	76.5

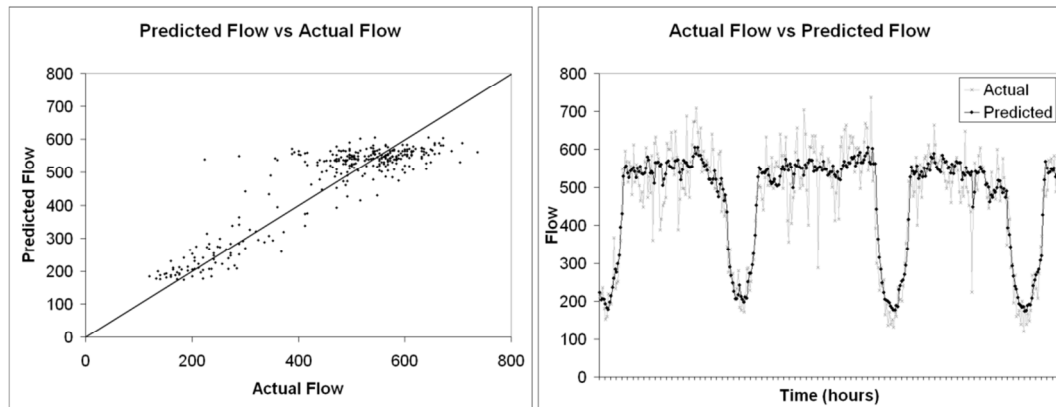


Figure 6. Scatter plot and line graph for the actual and predicted flow values for +15 minute prediction ($t+1$) for AURA k-NN configuration 1-6.

The prediction results for configuration (1-6) are plotted in figures 6 and 7 against the actual data values. The scatter plot and line graphs in figure 6 show the prediction accuracy for +15 minute prediction and the graphs in figure 7 show the prediction accuracy for +1 hour prediction. This illustrates where the prediction is accurate and where it is inaccurate across the time span of the test data. From figures 6 and 7, the AURA k-NN tends to smooth transient spikes, particularly transient spikes where the flow values suddenly decrease supporting our earlier conclusion that configurations 1-6 and 1-7 overestimate more.

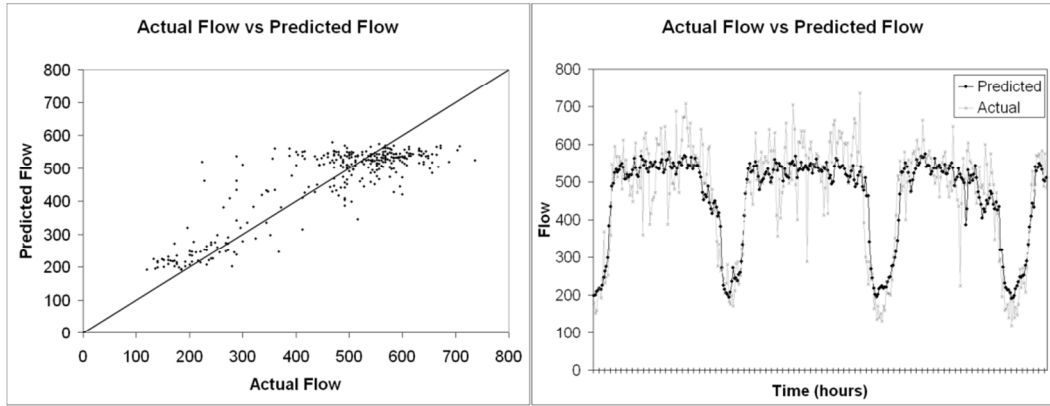


Figure 7. Scatter plot and line graph for the actual and predicted flow values for +1 hour prediction ($t+4$) for AURA k-NN configuration 1-6.

4.3.1 Test 3 – comparison to other algorithms

Next, we took the two best performing data configurations (1-6 and 1-7) from test 2 and compared AURA k-NN to the WEKA machine learning algorithms running these two data configurations.

- AURA k-NN and standard (WEKA) k-NN : $k=50$.
- MLP config 1.6: learning rate = 0.4, decay = true, momentum = 0.3
- MLP config 1.7: learning rate = 0.5, decay = true, momentum = 0.4.
- SVM config 1.6: RBF Kernel, complexity = 50.0
- SVM config 1.6: RBF Kernel, complexity = 75.0.

The recall accuracy results for configuration (1-6) are listed in table 3 and the results for (1-7) are listed in table 4.

Table 3. Table comparing the recall accuracy of the various predictors with time series length 8, flow and occupancy attributes and predicted sensor excluded (six sensors) for test 4 part 1. The highest prediction accuracy for each row is shown in bold.

	<i>AURA k-NN_ 1-6</i>	<i>k-NN</i>	<i>MLP</i>	<i>SVM</i>	<i>LMS</i>
RMSE – 15 mins	65.3	65.3	68.1	69.4	69.9
RMSE – 60 mins	75.3	75.3	80.5	80.5	85.7

For configuration 1-6, the AURA k-NN and the standard k-NN were the joint best performing predictors for both +15 minute and +1 hour prediction compared to the other approaches.

Table 4. Table comparing the recall accuracy of the various predictors with time series length 8, flow attribute only and all sensors for test 4 part 2. The highest prediction accuracy for each row is shown in bold.

	<i>AURA k-NN_ 1-7</i>	<i>k-NN</i>	<i>MLP</i>	<i>SVM</i>	<i>LMS</i>
RMSE – 15 mins	65.2	65.3	68.8	67.8	69.2
RMSE – 60 mins	76.1	76.9	81.1	80.7	86.5

The AURA k-NN was the best performing for both +15 minute and +1 hour prediction for configuration 1-7, closely followed by the standard k-NN. The RMSE varied for all algorithms between this data configuration and the previous indicating that all algorithms need to optimise the data configuration

4.3.2 Test 4 – the best data and AURA k-NN configuration

The first test of the AURA k-NN for data set 2 was to evaluate different configurations to find the optimal configuration(s) for prediction. For Marylebone Rd, we ran a single algorithm/data configuration test as only flow data was available whereas Russell Sq. had both flow and occupancy. The results are given in table 5. We evaluated: whether to incorporate the attributes of the sensor whose flow is being predicted (*S*); the time series length (*TS*); the number of bins to use for quantisation (*Bins*); and, the *k* value for AURA k-NN (*k*).

Table 5. Table listing the MPE, MAPE and RMSE for various configurations of the AURA k-NN with time series length 8 using the full week of query data. 15 indicates +15 minute ahead prediction and 60 indicates + 1 hour ahead prediction. The highest prediction accuracy for each column is shown in bold.

<i>AURA k-NN Configuration</i>					<i>MPE</i>		<i>MAPE</i>		<i>RMSE</i>	
<i>Name</i>	<i>S</i>	<i>TS</i>	<i>Bins</i>	<i>k</i>	<i>15</i>	<i>60</i>	<i>15</i>	<i>60</i>	<i>15</i>	<i>60</i>
2-1a	Y	6	25	50	-1.0	-1.1	8.9	11.4	117.6	144.4
2-1b	Y	10	25	50	-1.2	-1.0	9.1	10.6	118.9	136.1
2-1c	Y	8	11	50	-1.2	-1.3	9.3	11.5	119.3	143.6
2-1d	Y	8	25	50	-1.1	-1.0	9.0	11.0	117.3	139.3
2-1e	Y	8	49	50	-1.1	-1.0	9.0	11.0	118.1	139.9
2-1f	N	8	25	50	-1.3	-1.2	9.5	11.3	125.4	144.8
2-1g	Y	8	25	10	-1.1	-0.6	8.7	10.0	115.9	131.7
2-1h	Y	8	25	25	-1.1	-0.7	8.8	10.3	115.1	134.8

Again, there is a clear difference between the best RMSE and worst RMSE for both +15 minute and +1 hour prediction. The overall best performing configuration for test 4 with respect to MPE, MAPE and RMSE was 2-1g which had some similar settings to the best performing configuration (1-7) from test 2 (Russell Sq. data). However, there are differences in the settings and these demonstrate that both the algorithm and data must be configured and evaluated against each data set if optimum performance is needed even for relatively similar data.

The graphs in figure 8 show the prediction accuracy for configuration (2-1g) for +15 minute prediction as a scatter plot and line graph and the graphs in figure 9 show the prediction accuracy for +1 hour prediction for configuration (2-1g) as both a scatter plot and a line graph. This illustrates where the prediction is accurate and where it is inaccurate across the time span of the test data.

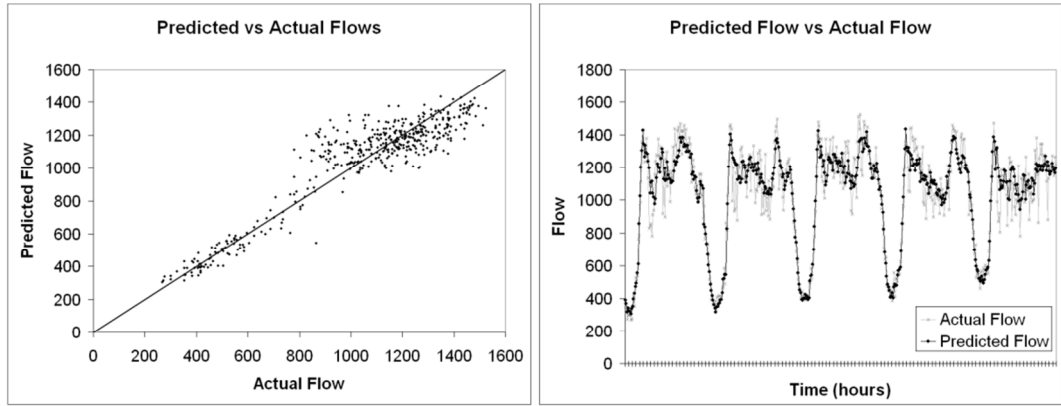


Figure 8. Scatter plot and line graph for the actual and predicted flow values for +15 minute prediction ($t+1$) for AURA k-NN configuration 2-1g.

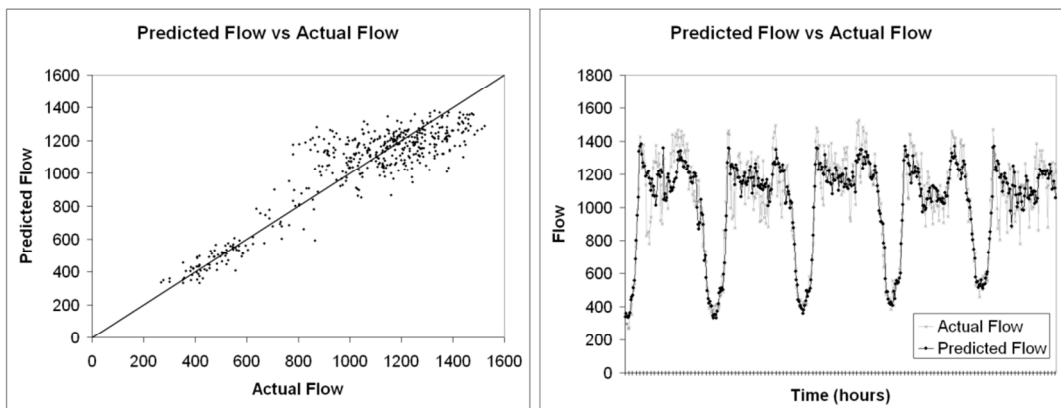


Figure 9. Scatter plot and line graph for the actual and predicted flow values for +1 hour prediction ($t+4$) for AURA k-NN configuration 2-1g.

From figures 8 and 9 and table 6, the AURA k-NN is again smoothing transient spikes.

4.3.3 Test 5 – the best configuration for incident detection

We repeated test 4 using the data for only the day of the traffic incident (20/06/08) which should be anomalous and thus more difficult to predict. The overall best performing configuration for test 5 with respect to MAPE and RMSE was identical to the best performing configuration for test 4. We call this test 5 configuration 2-2g. As the result replicated the result of test 4, the table of figures is omitted.

4.3.4 Test 6 – comparison to other algorithms

Test 6 compared AURA k-NN to the WEKA algorithms running identical data configurations on data set 2. The test comprised two parts. In part 1, we used configuration 2-1g from test 4 and the full week of test data. Part 2 used configuration 2-2g from test 5 and just the incident test data. The results for part 1 are listed in table 6 and for part 2 are listed in table 7.

- Standard k-NN: $k=10$ and $k=50$ (to verify that $k=10$ outperforms as per the AURA k-NN).
- MLP part 1 and part 2: learning rate = 0.4, decay = true, momentum = 0.3.
- SVM part 1: RBF Kernel, complexity = 150.0
- SVM part 2: RBF Kernel, complexity = 100.0.

Table 6. Table comparing the recall accuracy of the various predictors with time series length 8 and all sensors predicting a full week. The highest prediction accuracy for each row is in bold.

	<i>AURA k-NN_2-1g</i>	<i>k-NN_10</i>	<i>k-NN_50</i>	<i>MLP</i>	<i>SVM</i>	<i>LMS</i>
RMSE – 15 mins	115.9	115.6	117.8	114.6	116.3	123.6
RMSE – 60 mins	131.7	132.7	139.6	146.0	155.6	197.2

For part 1, the MLP had the lowest RMSE for +15 minute prediction followed by the k-NN_10 and AURA k-NN. For +1 hour prediction, AURA k-NN was the most accurate.

Table 7. Table comparing the recall accuracy of the various predictors with time series length 8 and all sensors predicting the day of incident only. The highest prediction accuracy for each row is shown in bold.

	<i>AURA k-NN_2-2g</i>	<i>k-NN_10</i>	<i>k-NN_50</i>	<i>MLP</i>	<i>SVM</i>	<i>LMS</i>
RMSE – 15 mins	128.8	128.0	137.8	137.5	142.4	161.9
RMSE – 60 mins	150.7	151.4	157.6	163.5	182.8	223.4

The standard k-NN performed best for part 2 for +15 minute prediction closely followed by the AURA k-NN and vice versa for +1 hour with AURA k-NN slightly outperforming.

For both evaluations, using $k=10$ outperformed using $k=50$ for the standard k-NN supporting our results for the AURA k-NN.

4.3.5 Test 7 – AURA k-NN run time.

Our final test was an analysis of the run time of AURA k-NN. It is vital that the underlying prediction algorithm is able to train and predict rapidly (between data collections) for on-line applications. Our preceding evaluations have confirmed that both the algorithm and the data must be configured. This configuration will need to be run periodically to maintain an up-to-date system and must be fast.

We have previously demonstrated that AURA k-NN training from raw data was up to four times faster than conventional k-NN [21]. Zhou et al. [38] determined that the AURA k-NN trains up to 450 times faster than an MLP. Training time is particularly important as this forms the bulk of the overall run time. Here we evaluated whether we can speed the AURA k-NN further by reading binary files from disk storage. The AURA

k-NN may read in the data as raw data and perform training of the CMM as per section 3. Alternatively, the contents of the CMM may be written to disk once the CMM has been trained and then read in from the saved file. We evaluated the timings for both approaches.

Table 8. Table listing the timings (seconds) for training the respective data sets from raw data, training the AURA k-NN from a stored CMM file and running a single query

Historical data size (vectors)	Train from raw (seconds)	Train from saved (seconds)	Query (seconds)
2,976	0.268	0.0020	0.0029
29,760	9.12	0.0169	0.0086
119,040	83.9	0.0662	0.0277
1,071,360	820.4	0.5914	0.2308

The software evaluated was a C++ prototype implementation that had not been optimised at this stage. It ran on a Linux-based 3.4Ghz Intel Pentium IV machine with 2GB of RAM and 1MB of cache. For this analysis, we used data set 2 training data comprising 2,976 records and applied one query of $TS=8$, $k=10$ and $Bins=25$. We then replicated the dataset ten times to give a training set of 29,760 records, forty times to produce 119,040 records and 360 times to produce 1,071,360 records and recorded the respective timings. The timings are averaged over five runs and are listed in table 8 and shown in figure 10.

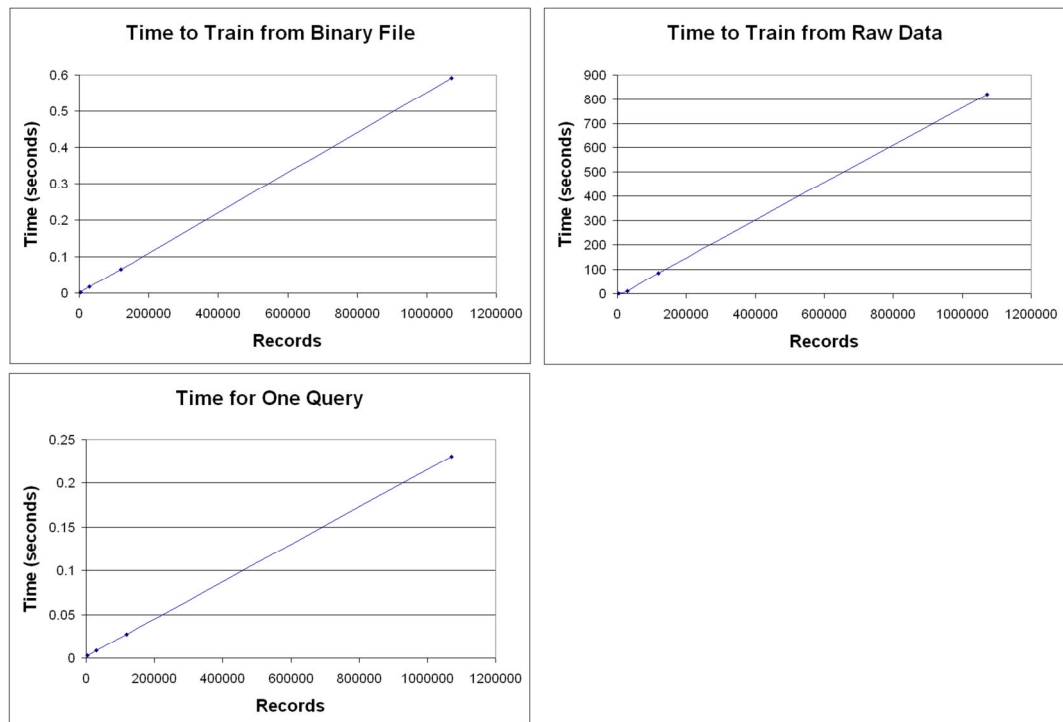


Figure 10. Graphs showing the actual growth in training time and query time from 2,976 to 1,071,360 records

The run time growth for AURA k -NN training and querying was linear: $O(n)$ which agrees with our theoretical figure established in section 3. Reading the data in from a CMM stored on disk can exploit the compact representation used for our CMM and is almost 1400 times faster compared to training from raw data for the large 1million+ records data set. We already knew that the AURA k -NN was up to four times faster than standard k -NN but reading the CMM from disk can further speed the AURA k -NN markedly.

Traffic data generally arrive at five minute intervals although they may arrive as frequently as every 30 seconds. One year of five minute interval data comprises 105,120 records. Interpolating from the above results, this would take approximately 0.07 seconds to read from the binary file and 0.04 seconds to query. Similarly, one year of 30 second interval data comprises 1,051,200 records which would take approximately 0.65 seconds to read from the binary file and 0.24 seconds to query. This timing analysis indicated that the AURA k -NN would be fast enough for our on-line IDS processing one year of historical data, typically producing results in less than one second.

5 Analyses

K -NN in general performs comparably with other modelling approaches here with respect to prediction accuracy as shown in tables 3, 4, 6 and 7. The advantage of the AURA k -NN lies in the speed and scalability of training and prediction.

For algorithm configuration, the AURA k -NN only needed to optimise the number of bins and the k value for each data set but these do need to be configured carefully and a range of values assessed. This agrees with both [19] and [20] where we also found that there is no single best k value for predicting bus journey times [19] or a single best number of bins for a broad range of time series data [20]. From the ten data sets evaluated in [20] and the traffic data sets evaluated here, there is no obvious correlation between the data characteristics and the best configuration neither is there an obvious correlation between the data distribution and the best configuration. Therefore, we aim to provide guidelines by recommending suitable ranges of values for k and the number of bins. We have found that the best k can range from 10 to 50 here. K -NN is an instance-based learner relying on the nearest stored data points to produce the prediction. The k value is affected by the density of the data and the data coverage. The k value needs to be set to ensure that the majority of points from the k best matches will predict the correct value. If the value is too low then the prediction is reliant on too few data points. If it is too high then it may draw data points from too large an area making prediction unreliable. The number of bins ranges from 11 to

49 here. If the number of bins is set too low then the AURA k-NN will fail to separate the data and discrimination will be too low. Too many bins and the data points become too sparse across multiple dimensions and fail to discriminate.

The CMM does not need to be retrained to optimise the k value as this just requires the number of matches returned to be varied. However, it does need retraining to optimise the number of bins. For data configuration: the sensors, the set of attributes from each sensor and the time series length all need to be optimised. Again, the CMM does not need retraining to vary the sensors or attributes. If all attributes that may be used are trained into the CMM then only CMM rows that relate to sensors under investigation need to be activated and all other rows may be ignored.

Using more spatially distributed sensors produced better prediction accuracy as shown by table 2 where AURA k-NN with 6 sensors outperforms AURA k-NN with 4 sensors with respect to MAPE and RMSE. Including the additional sensor attribute, occupancy, only improved the prediction accuracy marginally (see table 2) so additional attributes have to be selected carefully. Kamarianakis and Prastacos [18] showed that attributes and sensors need to be carefully considered and these results agree with their findings. Varying the time series length requires the CMM to be retrained. It was possible to pinpoint a single ideal time series length for both data sets here ($TS=8$) but we expect that the length would need to be varied for different data sets.

Previous evaluation have shown that AURA k-NN trains from raw data up to 450 times faster than an MLP [38] and executes up to four times faster than standard k-NN [21]. Here, we showed in table 8 that AURA k-NN executed even more rapidly by reading trained CMMs stored on disk and then retrieving the k nearest neighbours.

An advantage of both standard and AURA k-NN over the model-based approaches is that they can incorporate new data into the k-NN framework simply and quickly. New data may simply be added to the database for standard k-NN or added as new columns to the AURA CMM. A model-based approach would have to remodel the new data which is a computationally intensive process. The AURA k-NN will need to be tuned periodically to keep it up to date but evaluating multiple algorithm and data configurations is computationally feasible. Conversely, the SVM and MLP require intensive optimisation across a number of parameters and we noticed that the RMSE for both the SVM and the MLP varied according to the parameters selected. This presents computational processing issues for an on-line IDS using either an SVM or MLP as the data would need to be remodelled regularly as new data became available to prevent model drift.

We noted in our four criteria that the prediction algorithm must be able to accommodate non-stationary data and, thus, short-term data fluctuations. Mulhern and

Caprara [39] suggested that multivariate k-NN can identify chaotic time series patterns (such as those found in traffic flows) that model-based approaches would miss. The nonparametric regression technique of k-NN which effectively mines the data and retrieves actual cases (local search) is much better suited to such prediction tasks than data modelling techniques such as MLP, SVM or LMS which produce general models that tend towards the mean. Data such as traffic flows are susceptible to local, short-term variations such as daily variations in demand, incidents or the weather. These short-term variations must be identifiable by the technique to allow accurate prediction and a model that tends towards the mean may well miss them. This hypothesis agrees with the findings of [17, 39, 40] across various problem domains.

The AURA k-NN will generate a prediction using the average value of the k neighbours. This averaging tended to smooth transient spikes and appeared to be overestimating more frequently than underestimating for this data. However, the data sets used in these evaluations were relatively small. We posit that a larger training set, such as a full year of data with $365 * 96 = 35,040$ records (assuming no missing data), may lead to more accurate predictions as more examples of each time series would be present.

6 Conclusion

The AURA k-NN was the overall best performing predictor of the methods evaluated on the data sets in this paper in terms of both speed and accuracy. It performs comparably with respect to prediction accuracy and is able to be implemented for rapid execution and scalability of both training and retrieval of the k nearest neighbours. We envisage using the AURA k-NN as a “train once use many” predictor, writing the CMM to disk for safety, running repeated queries and reading the CMM from disk when necessary. New data may be added to the CMM by adding additional columns to the matrix. The rapid execution allows the algorithm and data parameters to be tuned if necessary to prevent drift.

All predictors evaluated here required both the data and algorithm settings to be configured. The fast execution time and minimal parameter set of the AURA k-NN facilitates this combinatorial configuration process. The only algorithm parameter required for standard k-NN is the k value. The AURA k-NN added one parameter to this: the number of quantisation bins for each attribute. It may be possible that heuristics to guide the parameter setting can be inferred through analysing a diverse range of data sets.

One disadvantage of k-NN is that it is only as good as the historical data in the database. Some model based methods such as MLPs are able to generalise and effectively plug gaps in the training data. If there is a gap in the data space then there will be no exemplars available to k-NN in this region so predictions will be produced from more

distant neighbours. Hence, it is vital, that the historical data base is sufficiently large with sufficient coverage to optimise accuracy. This is particularly true for infrequent events such as traffic incidents. A large database covering a long time span will contain more event data which will enable better instance-based prediction for a k-NN method. However, if the data base is too large then computational time will be excessive for standard k-NN. For this reason, we use the faster AURA k-NN to underpin the predictor so much larger databases with better coverage may be processed.

We feel that the AURA k-NN prediction accuracy can be improved. We noted from the MPE that the AURA k-NN tends to overestimate traffic flows. Hence, future work will investigate increasing the prediction accuracy by incorporating: time-of-day matching using time-of-day profiles; k-NN distance weighting; and, introducing error feedback. As discussed above, using a larger database covering a longer time span may also improve instance-based prediction. We will also investigate using confidence estimators where the prediction is accompanied by a confidence value based on the distance of the matches from the query.

Ultimately, it is hoped that the predictor will be incorporated into an intelligent decision support system for traffic monitoring and tested against real-world data from London, Kent and York in the UK. By producing predictions, the IDS will be able to make recommendations proactively and anticipate traffic problems rather than functioning reactively and being subject to time lags inherent in data collection. The proposed method is generic and we hope to apply it to other domains that use spatially distributed sensors where neighbourhoods of sensors exist and where temporal characteristics are important.

Acknowledgments

The work reported in this paper forms part of the FREEFLOW project, which is supported by the UK Engineering and Physical Sciences Research Council, the UK Department for Transport and the UK Technology Strategy Board. The project consortium consists of partners including QinetiQ, Mindsheet, ACIS, Kizoom, Trakm8, City of York Council, Kent County Council, Transport for London, Imperial College London and University of York.

References

- [1] Gorry, G. and Scott-Morton, M. (1971). A framework for management information systems. *Sloan Management Rev.*, 13(1):55-70.
- [2] Glover, P., Rooke, A. and Graham, A. (2008). Flow diagram. *Thinking Highways*, 3(3), pp. 20-23.

- [3] Schelter, B., Winterhalder, M. and Timmer, J. (2006). Handbook of time series analysis: recent theoretical developments and applications, Wiley-VCH, ISBN: 978-3-527-40623-4
- [4] Ding, A., Zhao, X. and Jiao, L. (2002). Traffic Flow Time Series Prediction Based On Statistics Learning Theory. In, Procs IEEE 5th International Conference on Intelligent Transportation Systems, pp. 727-730.
- [5] Vapnik, V. (1995). The nature of statistical learning theory. New York: Springer-Verlag, ISBN: 0387987800.
- [6] Box, G. and Jenkins, G. (1976). Time Series Analysis: Forecasting and Control. Holden-Day, San Francisco.
- [7] Hamed, M. and Al-Masaeid, H. (1995). Short-term prediction of traffic volume in urban arterials. J. of Transp. Eng. (ASCE) 121(3): 249-254.
- [8] Williams, B., Durvasula, P. and Brown, D. (1998). Urban freeway traffic flow prediction: Application of seasonal autoregressive integrated moving average and exponential smoothing models. Transp. Res. Record: J. of the Transp. Res. Board, 1644: 132-141.
- [9] Ghosh, B., Basu, B. and O'Mahony, M. (2007). Bayesian time-series model for short-term traffic flow forecasting. Journal of Transp. Eng. (ASCE) 133(3): 180-189.
- [10] Amin, S., Rodin, E., Liu, A-P. and Rink, K. (1998). Traffic Prediction and Management via RBF Neural Nets and Semantic Control. J. of Computer-Aided Civ. and Infrastruct. Eng., 13: 315-327.
- [11] Vlahogianni, E., Karlaftis, M. and Golias, J. (2005). Optimized and meta-optimized neural networks for short-term traffic flow prediction: A genetic approach. Transp. Res. Part C: Emerging Technologies, 13(3): 211-234.
- [12] Abdulhai, B., Porwal, H. and Recker, W. (2002). Short-Term Traffic Flow Prediction Using Neuro-Genetic Algorithms. J. of Intell. Transp. Sys.: Technology, Planning, and Operations, 7(1): 3-41: Taylor & Francis.
- [13] Martinez, T., Berkovich, S. and Schulten, K. (1993). Neural-gas network for vector quantization and its application to time-series prediction. IEEE-Trans. on Neural Netw., 4(4): 558-569.
- [14] Zhang, C., Sun, S. and Yu, G. (2004). Short-Term Traffic Flow Forecasting Using Expanded Bayesian Network for Incomplete Data. In, Procs International Symposium on Neural Networks, Dalian, China. Lecture Notes in Computer Science, (LNCS 3174), Springer-Verlag.
- [15] Kindzerske M. and Ni, D. (2007). A Composite Nearest Neighbor Nonparametric Regression to Improve Traffic Prediction. Transp. Res. Record: J. of the Transp. Res. Board, 1993: 30-35.
- [16] Yakowitz, S. (1987). Nearest-Neighbour Methods for Time Series Analysis. J. of Time Series Anal., 8(2): 235-247.
- [17] Krishnan, R. and Polak, J. (2008). Short-term travel time prediction: An overview of methods and recurring themes. Procs Transportation Planning and Implementation Methodologies for Developing Countries Conference (TPMDC 2008), Mumbai, India, December 3-6, 2008. CD-ROM

- [18] Kamarianakis, Y. and Prastacos, P. (2003). Forecasting traffic flow conditions in an urban network: Comparison of multivariate and univariate approaches. *Transp. Res. Record: J. of the Transp. Res. Board*, 1857: 74-84.
- [19] Hodge, V., Jackson, T. and Austin, J. (2012). A Binary Neural Network Framework for Attribute Selection and Prediction. In, *Procs 4th International Conference on Neural Computation Theory and Applications (NCTA 2012)*, pp. 510-515, Barcelona, Spain: SciTePress
- [20] Hodge, V. and Austin, J. (2012). Discretisation of Data in a Binary Neural k-Nearest Neighbour Algorithm. Tech Report YCS-2012-473, Department of Computer Science, University of York, UK
- [21] Hodge, V. and Austin, J. (2005). A Binary Neural k-Nearest Neighbour Technique. *Knowl. and Inf. Sys.*, 8(3): 276–292, Springer-Verlag London Ltd.
- [22] Austin, J., Kennedy, J. and Lees, K. (1998). The Advanced Uncertain Reasoning Architecture, AURA. In, *RAM-based Neural Networks*, Ser. Progress in Neural Processing. World Scientific Publishing, 9: 43-50.
- [23] Hodge, V., Krishnan, R., Austin, J. and Polak, J. (2010). A computationally efficient method for online identification of traffic incidents and network equipment failures. Presented at, 3rd Transport Science and Technology Congress: TRANSTEC 2010, New Delhi, April 4-7, 2010.
- [24] Krishnan, R., Hodge, V., Austin, J. and Polak, J. (2010a) A Computationally Efficient Method for Online Identification of Traffic Control Intervention Measures. 42nd Annual UTSG Conference, Centre for Sustainable Transport, University of Plymouth, UK: January 5-7, 2010
- [25] Krishnan, R., Hodge, V., Austin, J., Polak, J. and Lee, T-C. (2010b). On Identifying Spatial Traffic Patterns using Advanced Pattern Matching Techniques. In, *Transportation Research Board (TRB) 89th Annual Meeting*, Washington, D.C., January 10-14, 2010. (DVD-ROM: 2010 TRB 89th Annual Meeting: Compendium of Papers)
- [26] Hebb, D. (1949). *The organization of behavior: a neuropsychological theory*, Wiley, New York.
- [27] Hodge, V. and Austin, J. (2001). An evaluation of standard retrieval algorithms and a binary neural approach. *Neural Netw.*, 14(3): 287-303
- [28] Bentz, H., Hagstroem, M. and Palm, G. (1989). Information storage and effective data retrieval in sparse matrices. *Neural Netw.*, 2(4): 289–293.
- [29] Austin, J. (1995). Distributed associative memories for high speed symbolic reasoning. In, R. Sun and F. Alexandre, (eds), *IJCAI '95 Working Notes of Workshop on Connectionist-Symbolic Integration: From Unified to Hybrid Approaches*, pp. 87–93, Montreal, Quebec.
- [30] Weeks, M., Hodge, V., O'Keefe, S., Austin, J. & Lees, K. (2003). Improved AURA k-Nearest Neighbour Approach. In, *Procs IWANN-2003, International Work-conference on Artificial and Natural Neural Networks*, Mahon, Spain. June 3-6, 2003. *Lecture Notes in Computer Science (LNCS) 2687*, Springer Verlag, Berlin.
- [31] Hall, M., Frank, E., Holmes, G., Pfahringer, B., Reutemann, P. and Witten I. (2009). The WEKA Data Mining Software: An Update. *ACM SIGKDD Explorations Newsletter*, 11(1): 10-18.
- [32] Witten, I. and Frank, E. (2005). *Data Mining: Practical Machine Learning Tools and Techniques*, Second Edition. Morgan Kaufmann Publishers Inc., San Francisco, CA, USA.

- [33] Cover T. and Hart P. (1967). Nearest neighbor pattern classification. *IEEE Trans on Information Theory*, 13(1): 21–27.
- [34] Rumelhart, D., Hinton, G. and Williams, R. (1988). Learning representations by back-propagating errors (pp. 696-699). MIT Press, Cambridge, MA, USA.
- [35] Platt, J. (1998). Fast Training of Support Vector Machines using Sequential Minimal Optimization. In, B. Schoelkopf, C. Burges and A. Smola, (eds), *Advances in Kernel Methods - Support Vector Learning*. MIT Press, Cambridge, MA, USA, 185-208.
- [36] Labeeuw, W., Driessens, K., Weyns, D., Holvoet, T. and Deconinck, G. (2009). Prediction of Congested Traffic on the Critical Density Point Using Machine Learning and Decentralised Collaborating Cameras. In, *New Trends in Artificial Intelligence, 14th Portuguese Conference on Artificial Intelligence, EPIA 2009, Aveiro, Portugal*, pp. 15-26.
- [37] Krishnan, R., (2008). Travel time estimation and forecasting on urban roads, PhD thesis, Centre for Transport Studies, Imperial College London.
- [38] Zhou, P., Austin, J. and Kennedy, J. (1999). High Performance k-NN Classifier Using a Binary Correlation Matrix Memory. In, *Procs Advances in Neural Information Processing Systems Vol. II*, David A. Cohn (Ed.). MIT Press, Cambridge, MA, USA, 713-719.
- [39] Mulhern, F. and Caprara, R. (1994). A Nearest Neighbor Model for Forecasting Market Response. *Int. J. of Forecast.*, 10(2): 191-207, ISSN 0169-2070.
- [40] Oswald, R., Scherer, W. and Smith, B. (2001). Traffic Flow Forecasting Using Approximate Nearest Neighbour Nonparametric Regression. Research Report No. UVACTS-15-13-7. Centre for Transportation Studies, University of Virginia.

Appendix

WEKA MLP configuration.

Settings in *italic* were changed from the WEKA defaults but not changed between runs and settings in ***bold/italic*** were varied for each run to tune the MLP.

gui	false
autoBuild	true
debug	false
<i>decay</i>	<i>true</i>
<i>hiddenLayers</i>	<i>t (number of hidden layers = numAttribs + numClasses)</i>
<i>learningRate</i>	<i>0.4</i>
<i>momentum</i>	<i>0.3</i>
nominalToBinaryFilter	true
normalizeAttributes	true
normalizeNumericClass	true
reset	true
seed	0
trainingTime	500
<i>validationSetSize</i>	<i>30</i>
validationThreshold	20

WEKA SVM configuration.

Settings in *italic* were changed from the WEKA defaults but not changed between runs and settings in ***bold/italic*** were varied for each run to tune the SVM.

<i>complexity</i>	<i>50.0</i>
debug	false
<i>fileType</i>	<i>Normalize training data</i>
<i>kernel</i>	<i>RBFKernel -C 250007 -G 0.01</i>
regOptimizer	RegSMOImproved -L 0.0010 -W 1 -P 1.0E-12 -T 0.0010 -V